

# MrGCN: Mirror Graph Convolution Network for Relation Extraction with Long-Term Dependencies

Xiao Guo<sup>1\*</sup>, I-Hung Hsu<sup>1\*</sup>, Wael AbdAlmageed<sup>1</sup>, Premkumar Natarajan<sup>1</sup>, Nanyun Peng<sup>1,2</sup>

<sup>1</sup> Information Sciences Institute, University of Southern California

<sup>2</sup> Computer Science Department, University of California, Los Angeles

{xiaoguo, ihunghsu, wamageed, pnataraj} @isi.edu;  
violetpeng@cs.ucla.edu

## Abstract

The ability to capture complex linguistic structures and long-term dependencies among words in the passage is essential for many natural language understanding tasks. In relation extraction, dependency trees that contain rich syntactic clues have been widely used to help capture long-term dependencies in text. Graph neural networks (GNNs), one of the means to encode dependency graphs, has been shown effective in several prior works. However, relatively little attention has been paid to the *receptive fields* of GNNs, which can be crucial in tasks with extremely long text that go beyond single sentences and require discourse analysis. In this work, we leverage the idea of *graph pooling* and propose the Mirror Graph Convolution Network (MrGCN), a GNN model with pooling-unpooling structures tailored to relation extraction. The pooling branch reduces the graph size and enables the GCN to obtain larger *receptive fields* within less layers; the unpooling branch restores the pooled graph to its original resolution such that token-level relation extraction can be performed. Experiments on two datasets demonstrate the effectiveness of our method, showing significant improvements over previous results.

## 1 Introduction

Relation extraction (RE), a task to extract the relation between entity in the text, serves as an important intermediate step in various tasks in natural language processing (NLP). While earlier works in RE focus on binary relations (relations that only involve two entities) within a single sentence (Miwa and Bansal, 2016), recent works place more emphasis on identifying the relation between entities that appear in different sentences or require a large context to disambiguate (Gupta et al., 2019; Akimoto et al., 2019). For example, Peng et al. (2017) study relation extraction for  $n$  ( $n \geq 2$ ) entity mentions

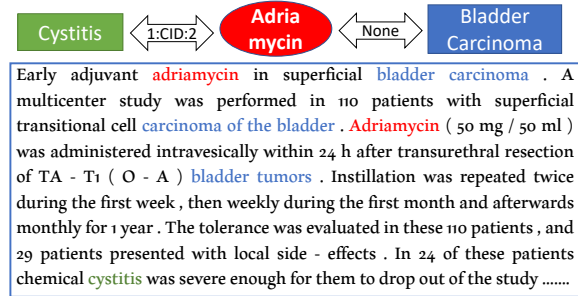


Figure 1: Example of document-level relations from the CDR dataset. The oval refers to chemical **Adriamycin**, and the rectangles represent two diseases, **Bladder Carcinoma** and **Cystitis**. It is necessary to read the whole passage to understand the relation between **Adriamycin** and **Cystitis**.

( $n$ -ary relation) spanning multiple sentences (cross-sentence), and Li et al. (2016a) provide a chemical-disease reactions (CDR) dataset that annotates binary relations between entities at *document-level*.

Though these settings are more general and practical, they bring special challenges to machine learning models. Most notably, the models need to capture *long-term dependencies* between words to better capture relations between entities spanning several sentences. Taking Figure 1 as an example, the relation between **Cystitis** and **Adrimycin** can only be understood by considering the whole paragraph over six sentences.

To address the long-term dependency challenges in RE, prior works incorporate dependency trees to capture non-local syntactic clues to supplement the surface form (Miwa and Bansal, 2016; Zhang et al., 2018). Graph neural networks (GNNs), one way to encode the syntactic and discourse information of the input text, has been widely explored (Peng et al., 2017; Sahu et al., 2019). However, the *receptive fields* (Luo et al., 2016) of GNNs, which measure the information range that an node in a graph can access, are less discussed in works that apply GNNs to NLP tasks. Intuitively, enlarging the *receptive*

\* The authors contribute equally, alphabetical order.

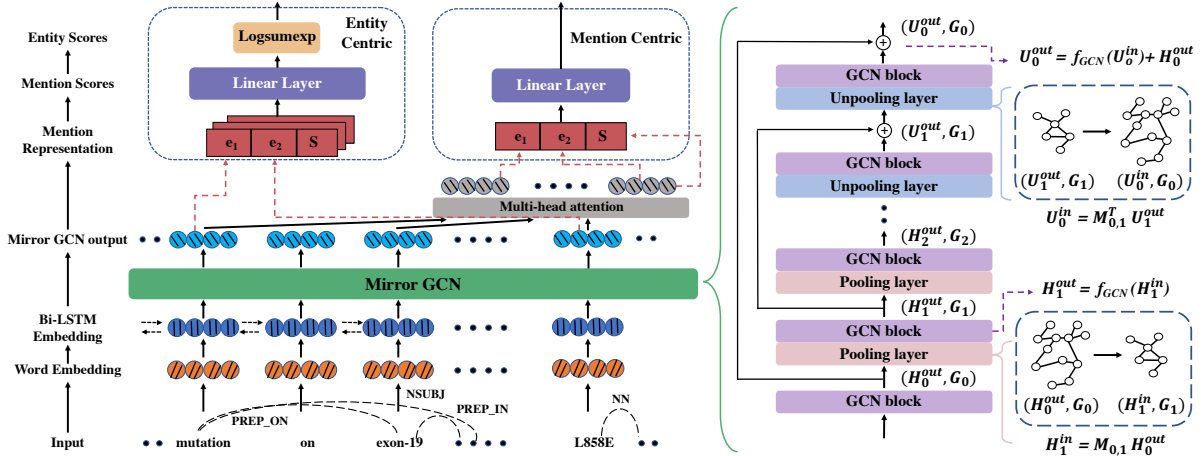


Figure 2: Mirror Graph Convolutional Network (MrGCN) for RE tasks. **Left:** The overall architecture: the **word embeddings** from the input text are fed to the Bi-LSTM layer and **Mirror GCN** to learn representations for each token. The **output features** are then used for the entity-centric or mention-centric RE. **Right:** Details of **Mirror GCN**. Input graph embeddings flow through a GCN block, several pooling layers and unpooling layers to aggregate information with different scales.  $G_i$  represents hypergraphs at the  $i$ -th level.  $H_i^{in}$  and  $U_i^{in}$  denote the converted embeddings after the pooling and unpooling layers in  $i$ -th hypergraph using the matching matrix  $M_{l,l+1}$  and the residual connections.  $H_i^{out}$  and  $U_i^{out}$  are the refined representations after GCN blocks.

field of GNNs is essential to learn representation that can capture extremely long-term dependencies between words.

Inspired by the recent development of *graph pooling* with a pooling-unpooling structure in GNNs for graph representation learning (Gao and Ji, 2019; Yu et al., 2019), we adapt the idea and propose a Mirror Graph Convolutional Network (MrGCN), which has a symmetric architecture with the pooling-unpooling mechanism and is tailored to RE. More formally, the pooling branch helps the model learn a larger *receptive field* for each graph node than the vanilla GCN with the same number of layers, and the unpooling branch restores the pooled graphs to the original graph such that token-level RE can be performed.

Specifically, we use *Graph Pooling* to convert the input document graph (Quirk and Poon, 2016) to a series of more compact hypergraphs by merging structurally similar or related nodes into *supernodes*. Each *supernode* serves as an information union of corresponding children nodes. The graph convolution operation on the hypergraphs thus aggregates a larger neighborhood of features, increasing the size of the *receptive field* for each node. As depicted in Figure 2, we perform neighborhood aggregations via GCN blocks to learn node representations at each level. Unpooling layers then restore global information from *supernodes* back to their corresponding children nodes. With this

pooling-unpooling mechanism, each graph node obtains richer features.

We benchmark MrGCN on two RE tasks and achieve new state-of-the-art (SOTA) results. To understand the effectiveness of *graph pooling*, we conduct comprehensive ablation studies and propose a novel analysis that examine the model performance against distances among entities in the input graph. These studies show that *graph pooling* helps improving the model performance significantly when long-term dependencies are required.

Our contributions are threefold: (1) We propose MrGCN to tackle the problem of discourse-level RE. Our model flexibly handles two variants of RE tasks and is agnostic to the graph pooling strategies; (2) We systematically study the graph pooling-unpooling mechanism for GNNs on RE tasks and achieve SOTA results on two datasets; (3) We conduct comprehensive analyses and propose a novel way to show MrGCN’s ability on handling relations between entities with long distances in graph.

## 2 Background

**Task Definition.** There are two typical RE tasks, mention-centric RE and entity-centric RE. Mention-centric RE predicts relation  $R$  of given entity mentions,  $e_1, \dots, e_n$ , in the context  $T$ . Entity-centric RE focuses on identifying the relation  $R$  among  $E_1, \dots, E_m$  from the context  $T$ , in which  $E_i$  indicates an entity and each entity can have multi-

ple mentions in  $T$ . For example, entity *adriamycin* has been mentioned multiple times in Figure 1. Both RE tasks can be formulated as classification tasks and we study both of them in this paper.

**Document Graph.** Document graph (Quirk and Poon, 2016) represents intra- and inter-sentential dependencies in texts. It consists of nodes representing words and edges representing various dependencies among words. Typically, two words can be linked if they (1) are adjacent, (2) have dependency arcs, or (3) share discourse relations, such as coreference or being roots of sequential sentences. In this paper, we view the document graphs undirected and apply our model to them for leveraging syntactic and discourse clues of the input text.

### 3 Proposed Method

Figure 2 depicts the proposed MrGCN model. Input texts are first encoded into contextualized embedding via word embedding and BiLSTM layers, and then fed into Mirror GCN to learn representations for each token. Depending on the RE task, the token representation will be used differently to make the final predictions. We will first give an overview of our model and then provide more details about each component.

#### 3.1 Overview

Mirror GCN is designed with a pooling-unpooling structure. The pooling layer deterministically converts a graph into a more compact *hypergraph* using *matching matrices* and we explored several pooling strategy in (Section 3.2). A GCN block is then employed to update the graph embeddings for each pooled hypergraph (Section 3.3). After several levels of pooling and representation learning, the unpooling layer performs a reverse operation to the pooling layer that restores finer-grain graphs from the hypergraphs (Section 3.4). It is mirrored because the same layers of unpooling will be applied assembling the pooling layers to restore the original graph from the coarsest-grain hypergraph. Node embeddings in each level of the unpooled graphs will also be updated by GCN blocks. RE models are then built on top of the final node representation to perform the final task (Section 3.5).

#### 3.2 Graph Pooling

The idea of *graph pooling* is commonly used for graph representation learning tasks, which iteratively coarsens graph  $G$  into a smaller but struc-

turally similar graph  $G'$ . It usually first discovers nodes that can be matched as the same group based on different strategies (Ying et al., 2018; Lee et al., 2019). Then, nodes that are matched will be merged into a *supernode*. We explore two graph pooling strategies, *Common Head Matching* and *Hybrid Matching*.

**Common Head Matching (CHM).** We propose CHM, an intuitive method that leverages the hierarchical structure of the dependency tree from the input text. More formally, based on the dependency tree for each sentence, CHM matches nodes that share the same parent node to facilitate the information communication between nodes residing in different branches. For example, in Figure 3a, node  $n_3$  (*Drug-C*) and  $n_5$  (*Syndrome-B*) are merged into a group by CHM, as they share the common parent node  $n_4$  (*treats*). Likewise,  $n_6$  (*and*) and  $n_7$  (*Syndrome-D*), and  $n_0$  (*Disease-A*) and  $n_2$  (*Syndrome-B*) are merged into groups. After pooling using CHM, the distance between  $n_3$  and  $n_7$  decreases, hence facilitating the information exchange between these two nodes.

**Hybrid Matching.** Hybrid Matching (Liang et al., 2018) is shown to be effective for learning large-scale graph embeddings. Compared to CHM which only considers the depth information in the dependency tree, it considers the overall structural information of the document graph. It consists of two-stages: *structural equivalence matching* (SEM) and *normalized heavy edge matching* (NHEM).

SEM merges two nodes that share the exact same neighbors into a supernode. In the example illustrated in Figure 3b, node  $n_0$  (*Disease-A*) and  $n_2$  (*Syndrome-B*) are considered as structural equivalence, since they share the exact same and the only neighbor node  $n_1$  (*causes*).

In NHEM, we first calculate the *normalized edge weight*,  $W(u, v)$ , for each edge in the graph:

$$W(u, v) = \frac{A_{uv}}{\sqrt{D(u) \times D(v)}}. \quad (1)$$

$D(u)$  is the degree of node  $u$  and  $A_{u,v}$  represents the weight on edge between node  $u$  and  $v$ . In terms of computing edge weight  $A_{u,v}$ , we first initialize the weighted adjacency matrix  $A_0$  where each cell value is either 1 or 0, indicating if a connection exists or not. Then we employ Equation 3 to update the weighted adjacency matrix in the hypergraph. More details can be found in the appendix.

We visit nodes by ascending order according to the node degree in NHEM, and match each node

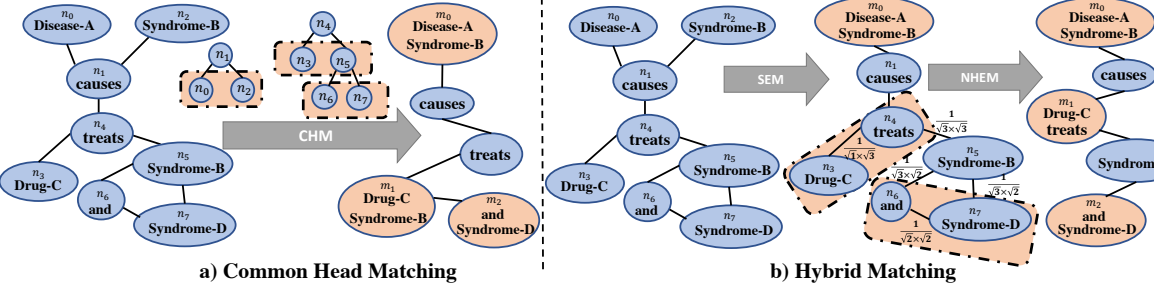


Figure 3: An illustration of two pooling methods. Given the instance “Disease-A causes Syndrome-B. Drug-C treats Syndrome-B and Syndrome-D”, where target entities are “Disease-A”, “Drug-C” and “Syndrome-D”, we first create the corresponding document graph which contains adjacent links, dependency arcs and the discourse relations. **Left:** *Common head matching* (CHM), which merges nodes with the same parent node based on the dependency trees. As a result, the distance between “Drug-C” and “Syndrome-D” decreases by 2. **Right:** *Hybrid matching*, which contains SEM and NHEM. After performing this pooling algorithm, the distances from “Drug-C” to “Disease-A”, and from “Drug-C” to “Syndrome-D” decrease by 1.

with its neighbor that has the largest *normalized edge weight* (NEW). This process is demonstrated in Figure 3b. After computing NEW, we first visit node  $n_3$  (*Drug-C*) whose degree equals 1, and merge it with its only neighbor  $n_4$  (*treats*) into the supernode  $m_1$  (*Drug-C, treats*). Then, we visit node  $n_6$  (*and*), whose has a neighbor  $n_7$  (*Syndrome-D*) with the largest NEW. Hence, we merge  $n_6$  (*and*) and  $n_7$  (*Syndrome-D*) into a supernode  $m_2$  (*and, Syndrome-D*). Also, it is worth noting that, as with Liang et al. (2018), supernodes cannot be merged again in each round of the Hybrid Matching, which explains why neither  $n_1$  (*causes*) nor  $n_5$  (*Syndrome-B*) is merged with other nodes. It can be observed that distances from “Drug-C” to “Disease-A”, and from “Drug-C” to “Syndrome-D” are shortened after Hybrid Matching.

**Pooling Operation.** We generate a coarsened hypergraph after each matching process. It means performing matching  $L$  times produces  $L$  hypergraphs with increasing coarsening levels, denoted as  $G_0, G_1, \dots, G_L$ , where  $G_0$  is the initial graph. We use *matching matrix*  $M_{l-1,l}$  to mathematically represent the matching process from level  $l-1$  to level  $l$ . Matching matrix  $M_{l-1,l} \in \mathbb{R}^{n \times m}$  converts  $G_{l-1} \in \mathbb{R}^{n \times n}$  to  $G_l \in \mathbb{R}^{m \times m}$  with  $n \geq m$ . Each cell  $m_{i,j}$  in  $M_{l-1,l}$  is:

$$m_{i,j} = \begin{cases} 1, & \text{if node } i \text{ is matched into supernode } j. \\ 0, & \text{otherwise.} \end{cases} \quad (2)$$

With  $M_{l-1,l}$  constructed, we can compute the weighted adjacency matrix of level  $l$  ( $A_l$ ) based on that of level  $l-1$ :

$$A_l = M_{l-1,l}^T A_{l-1} M_{l-1,l} \quad (3)$$

and perform representation transformation to get the *initial* node embeddings for the next level:

$$H_l^{in} = M_{l-1,l} H_{l-1}^{out} \quad (4)$$

where  $H_{l-1}^{out}$  and  $H_l^{in}$  represent the output embedding of  $G_{l-1}$  and the input embedding of  $G_l$ .

### 3.3 Graph Convolutional Network

Given the hypergraphs that we have generated through graph pooling, graph convolution is executed to update node embeddings on the hypergraphs. GCN (Kipf and Welling, 2016) is an extension of Convolutional Neural Network (LeCun et al., 1998) for non-euclidean graphs. The GCN block in our model is a stacked GCN with  $S$  layers ( $S \in \mathbb{Z}^+$ ), and for simplicity, we do not adopt complex techniques in our GCN block, such as incorporating directionality or edge-wise gates (Bastings et al., 2017; Marcheggiani and Titov, 2017).

With the adjacency matrix  $A$  we introduced before, the operation of the GCN block becomes:

$$h_i^l = \text{RELU} \left( \sum_{j=1}^N A_{[i,j]} W^l h_j^{l-1} + b^l \right), \quad (5)$$

where  $h_i^l$  is the representation of node  $i$  in the  $l$ th graph, and  $W^l$  and  $b^l$  are the corresponding weight and bias term. We define the output embedding  $H_l^{out}$  of  $G_l$  as  $H_l^{out} = f_{GCN}(H_l^{in})$ , where  $f_{GCN}$  approximates the GCN block function.

### 3.4 Graph Unpooling

After levels of graph pooling, MrGCN encodes information with enlarged receptive field into the coarsest-grain hypergraph. The unpooling branch

then restores and refines the information to the original resolution for downstream tasks.

Specifically, the unpooling layers use the matching matrix from the pooling layers and perform reverse operations, including generating larger graphs and mapping the embeddings to unpooled graphs. Each unpooling layer is followed by a GCN block to finetune representations. We denote the unpooling operation on  $l$ th graph embedding as:

$$U_{l-1}^{in} = M_{l-1,l}^T U_l^{out}, \quad \widetilde{U}_{l-1}^{out} = f_{GCN}(U_{l-1}^{in}). \quad (6)$$

Additionally, we add the residual connection to perform element-wise summation from corresponding embeddings in pooling branch as depicted in Figure 2, i.e.  $U_{l-1}^{out} = \widetilde{U}_{l-1}^{out} + H_{l-1}^{out}$ . This operation not only combines information at different scales but also prevents the architecture from potential degradation with increasing layers (He et al., 2016).

MrGCN can help model long-term dependencies because of the *pooling-unpooling paradigm*: performing graph convolution on supernode embeddings in the pooling branch will largely increase the information range that each node can access, while the unpooling branch is designed to refine embedding with different scales and restore information to each token in the original graph. It is also worth mentioning that our model design is *agnostic to the graph pooling method* and flexible to be extended.

### 3.5 Apply to Relation Extraction

The node embeddings obtained from MrGCN encoded comprehensive contextual features for each token in the input sample. In this section, we introduce ways of applying such features to mention-centric and entity-centric RE tasks.

**Mention-centric RE.** We first add an additional multi-head self-attention layer to perform a final refinement for each token representation. The embeddings of tokens that are entity mentions are concatenated with the additional max-pooled sentence embedding, and then fed into linear layers for the final classification. Figure 2 illustrates the whole process.

**Entity-centric RE.** In entity-centric RE, only relation labels for entities are available. Due to the coarse-grained learning signal, it is difficult to evaluate the contribution of each mention pair in the text. To accumulate all the representations for each mention pair and produce per-relation score for the entity pair, we adopt the method from Verga et al. (2018); Jia et al. (2019) to use the LogSumExp

function as the smooth approximation of max pooling method to aggregate information from multiple mentions of the given entities:

$$score(E_1, E_2) = \log \sum_{e_1 \in E_1, e_2 \in E_2} \exp(g(e_1, e_2)), \quad (7)$$

where  $score(E_1, E_2)$  is the final logit for entity pair  $(E_1, E_2)$ , and  $g(e_1, e_2)$  is the score for the given mention tuple  $e_1$  and  $e_2$ <sup>1</sup>.

## 4 Experiments

Experiments are conducted on two RE datasets, the Cross-Sentence  $n$ -ary Dataset (Peng et al., 2017) and the Chemical-Disease Reactions Dataset (Li et al., 2016a). Our models are developed using PyTorch (Paszke et al., 2019) and SGD optimizer for training. Dataset statistics and best hyper-parameters ( $S$  layers of GCN in GCN block and level  $L$  of pooling times) are stated in the appendix.

### 4.1 Cross-Sentence $n$ -ary Dataset

**Data and Task Settings:** The cross-sentence  $n$ -ary dataset ( $n$ -ary) dataset contains drug-gene-mutation ternary and drug-mutation binary relations annotated via distant supervision (Mintz et al., 2009). For this dataset, we investigate two experimental setups: (1) *Entity Anonymity*, which replaces target entities with dummy tokens to prevent the classifier from simply memorizing the entity names. It is a standard practice in distant supervision RE (Jia et al., 2019); (2) *Entity Identity*, where all tokens are exposed to the model.<sup>2</sup>

**Implementation Details:** The document graph is provided in the original released  $n$ -ary dataset.<sup>3</sup> We follow previous measurements – average accuracy of 5-fold cross-validation,<sup>4</sup> and use GloVe vectors for word embeddings initialization (Pennington et al., 2014).

**Results on  $n$ -ary dataset:** Table 1 shows the performance comparison on the  $n$ -ary dataset. We

<sup>1</sup>We try multi-head self-attention in entity-centric model, but it works worse than the model without attention. Our hypothesis is that the learning signal in entity-centric tasks are too weak to learn extra parameters in the attention, especially in the case where long context needs to be considered.

<sup>2</sup>Prior works are inconsistent w.r.t. this experimental detail. Specifically, Peng et al. (2017) conducted experiments under *Entity Anonymity* setup, while Song et al. (2018) and Guo et al. (2019) reported results under *Entity Identity* setup. For fair comparisons, we report results under both settings.

<sup>3</sup>[www.github.com/VioletPeng/GraphLSTM\\_release](http://www.github.com/VioletPeng/GraphLSTM_release)

<sup>4</sup>We use the same data partition and the validation data setup with Song et al. (2018).

Model		Detection						Classification					
		Ternary			Binary			Ternary			Binary		
	Overall	Single	Cross	Overall	Single	Cross	Overall	Single	Cross	Overall	Single	Cross	
Anonym.	Graph LSTM	80.7	77.9	83.3	76.7	76.6	76.9	N/A	N/A	N/A	N/A	N/A	N/A
	AGGCN	76.7	77.6	76.4	79.0	80.3	77.9	67.5	67.1	67.6	67.9	67.0	68.9
	MrGCN(CHM)	<u>83.1</u>	80.9	<u>84.0</u>	80.6	<u>80.0</u>	81.3	<u>77.1</u>	71.1	<u>79.6</u>	<u>76.2</u>	73.6	<u>78.1</u>
	w/o BiLSTM	81.1	79.4	81.6	80.2	79.6	<u>81.3</u>	74.3	70.0	76.1	73.5	72.3	74.4
	MrGCN(Hybrid)	<b>83.6</b>	81.3	<b>84.4</b>	<b>81.4</b>	80.0	<b>82.6</b>	<b>78.3</b>	<b>73.3</b>	<b>80.2</b>	<b>76.5</b>	<b>74.4</b>	<b>78.2</b>
	w/o BiLSTM	82.2	<b>83.2</b>	81.7	<u>80.8</u>	<b>80.4</b>	81.2	76.2	<u>72.2</u>	77.9	75.1	<u>74.0</u>	75.9
Identity	GS GLSTM	83.2	80.3	85.8	83.6	83.5	83.8	71.7	N/A	N/A	71.7	N/A	N/A
	GCN (Full Tree)	84.8	84.3	84.9	83.6	84.2	83.1	77.5	N/A	N/A	74.3	N/A	N/A
	AGGCN	87.0	87.1	86.9	85.6	85.2	86.2	79.7	N/A	N/A	77.4	N/A	N/A
	MrGCN(CHM)	90.2	89.1	90.5	93.4	93.5	93.3	<u>91.1</u>	89.7	91.5	94.1	93.8	94.3
	w/o BiLSTM	89.2	88.5	89.4	93.2	93.8	92.7	89.3	<u>90.9</u>	<u>94.4</u>	94.1	94.8	94.2
	MrGCN(Hybrid)	<b>91.6</b>	<u>91.0</u>	<b>91.7</b>	<b>94.1</b>	<b>94.5</b>	<b>93.8</b>	<b>91.3</b>	<b>92.6</b>	<b>95.3</b>	<b>95.3</b>	<b>95.4</b>	<b>95.3</b>
	w/o BiLSTM	<u>91.5</u>	<b>91.8</b>	<u>91.3</u>	<u>94.0</u>	<u>94.2</u>	<u>93.7</u>	90.8	90.0	91.2	94.7	<u>95.2</u>	94.3

Table 1: Results in average accuracy (%) of five-fold cross validation on the  $n$ -ary dataset for four sub-tasks. We compare our two variations, MrGCN(CHM) and MrGCN(Hybrid), with Graph LSTM (Peng et al., 2017) and AGGCN (Guo et al., 2019) in the *Entity Anonymity* (Anonym.) setting, and with GS GLSTM (Song et al., 2018), GCN (Full Tree) (Zhang et al., 2018), and AGGCN in the *Entity Identity* (Identity) setup. Instances in the whole  $n$ -ary dataset (denoted as Overall) contains instances that are either within a single sentence (denoted as Single) or across sentence boundaries (denoted as Cross).

report results of our method with two pooling variations, i.e, MrGCN(CHM) and MrGCN(Hybrid), representing MrGCN with common head matching pooling and with hybird matching, respectively. To fairly compare our method with baselines without BiLSTM, we also report the results from MrGCN ablating BiLSTM. We first compare our performance with prior works, GS GLSTM (Song et al., 2018), GCN (Full Tree) (Zhang et al., 2018)<sup>5</sup>, and AGGCN (Guo et al., 2019), under Entity Identity setup. As the lower part of Table 1 demonstrates, we outperform previous works by a large margin even without BiLSTM (at least 2.2% improvements in accuracy across all tasks). With the help of BiLSTM, our model can further improve the results.

Then, we compare MrGCN with Graph LSTM (Peng et al., 2017) and AGGCN (Guo et al., 2019)<sup>6</sup>. Results show that Hybrid Matching method performs better than CHM, yet both of our methods surpass the previous best results by at least 1.6% accuracy. Again, the superiority of our method holds even on models without BiLSTM, which have at least 1.2% improvement over prior works.

We report accuracy only on instances within single sentences (column *Single*) and that on instances with the entity pairs across sentence boundary (column *Cross*), which contain lengthier input context and require longer dependencies for models to consider. Our models have higher accuracies on *Cross*

<sup>5</sup>The result is adapted from Guo et al. (2019).

<sup>6</sup>The reported results of AGGCN in the upper of Table 1 are from our re-implementation by modifying their released code to make it match *Entity Anonymity* setup.

instances and gain the larger improvements over the baselines on these instances, which present an empirical evidence that our pooling-unpooling architecture successfully offers a way to model long-term dependencies.

## 4.2 Chemical-Disease Reactions Dataset

**Data:** The chemical-disease reactions dataset (CDR) was created from Comparative Toxicogenomics Database (CTD) (Davis et al., 2019), which only contains document-level labels between entities and do not contain mention information. The CDR dataset is a subset of CTD supplemented with human annotated mention span, forming CDR a entity-centric document-level RE task.

**Implementation Details:** Unlike the  $n$ -ary dataset, no document graph is provided in the original CDR datset, so we generate its document graphs similar to Sahu et al. (2019) using Stanford CoreNLP (Manning et al., 2014). Following Christopoulou et al. (2019), we use GENIA Sentence Splitter for sentence splitting, GENIA Tagger (Tsuruoka et al., 2005) for tokenization, and PubMed pre-trained word embeddings (Chiu et al., 2016). We follow (Christopoulou et al., 2019) to train the model in two steps. First, we train our model using standard training set and record the best number of epoch when the model reaches optimal on the validation set. Then, the model is re-trained using the union of the training and development data with the recorded number of epoch.

**Results on CDR dataset:** We apply our better

Model	P	R	F1
Gu et al.	55.7	68.1	61.3
Verga et al.	55.6	<b>70.8</b>	62.1
Nguyen and Verspoor	57.0	68.6	62.3
Christopoulou et al.	62.1	65.2	63.6
MrGCN(Hybrid)	<b>63.9</b>	65.6	<b>64.7</b>
Peng et al.	62.1	64.2	63.1
Li et al.	60.8	76.4	67.7
Verga et al. + Data	64.0	69.2	66.2

Table 2: Precision (P), recall (R), and F1 results on the test set in CDR. We compare MrGCN(Hybrid) model with SOTA models. Methods below the double line use additional training data.

performed model, MrGCN(Hybrid), on the CDR dataset, and the result is shown in Table 2. Some of the previous works include additional data in CTD dataset (Peng et al., 2016; Li et al., 2016b; Verga et al., 2018) as extra training data and achieved the best results on the CDR dataset. However, we do not use such data, thus, we compare our MrGCN(Hybrid) with models that do not incorporate additional data. As shown by the results, our MrGCN(Hybrid) model outperforms the current best model that uses only official data by 1.1 F1 scores and even outperform one of the baselines that uses external data.

## 5 Analysis and Discussion

In this section, we investigate how MrGCN benefits from its different components. Especially, in Section 5.2, 5.3, 5.4, we verify our hypothesis on that the idea of *Graph Pooling* can help model capture long-term dependencies more efficiently and effectively. The results provide supporting evidences that MrGCN performs well in scenarios where long-term dependencies are required.

We use our best approach, i.e, MrGCN(Hybrid), to conduct these analyses. It is noteworthy that Entity Anonymity setup is more principled when coping with the distant supervision dataset, so in this section, results on the *n*-ary dataset are obtained under *Entity Anonymity*.

### 5.1 Ablation Studies

We present ablation studies in Table 3. Comparing *MrGCN(Hybrid)-RNN* with *MrGCN(Hybrid)-RNN-pooling*, models with graph pooling benefit from enlarged receptive fields, and are consistently proven better. In the *n*-ary dataset, the improvements are at least 0.7 accuracy increase in 3 out of 4 sub-tasks. As for the CDR dataset, pooling brings 1.7 F1 scores boost. Likewise, ablating

Model	<i>n</i> -ary				CDR	
	Detection		Classification			
	Ter.	Bin.	Ter.	Bin.		
MrGCN(Hybrid)	<b>83.6*</b>	<b>81.4</b>	<b>78.3*</b>	<b>76.5</b>	<b>64.7*</b>	
-pool	81.2	81.2	76.8	76.2	62.7	
-RNN	82.2*	80.8*	76.2*	75.1*	61.9*	
-RNN-pool	82.0	80.1	73.8	70.0	60.2	
-RNN-pool-Att.	77.4	79.1	70.3	71.2	N/A	

Table 3: The ablation study of MrGCN(Hybrid). The reported values are measured in average accuracy (%) for *n*-ary dataset and F1 scores (%) for CDR dataset. Ter. and Bin. are abbreviations for ternary and binary relation, respectively. There is no multi-head attention (Att.) component for models in the entity-centric dataset (e.g. CDR), hence, the setting in the last row is N/A for CDR. \* indicates the model outperforms its corresponding model without pooling with p-value < 0.01 per McNemar’s test.

ing pooling (*MrGCN(Hybrid)-pooling*) from full *MrGCN(Hybrid)* leads performance decreases, especially over CDR dataset in which the difference is 2.0 F1 scores. As the ablation studies show, the benefits brought by the pooling mechanism is more significant on the CDR dataset and *n*-ary dataset’s ternary cases. We hypothesize the reason being that instances in CDR dataset and *n*-ary ternary cases have the longer distance, which can further highlight the importance of the pooling-unpooling mechanism to handle complex cases.

BiLSTM layers are useful in both datasets. This can be observed by comparing results from *MrGCN(Hybrid)* and from *MrGCN(Hybrid)-RNN*, where removal of BiLSTM causes the performance drop. As we know, GCN is relatively incapable of carrying sequential information in the context, which is crucial to learn the semantics. Conversely, BiLSTM’s contextualized embeddings provide us a way to learn such sequential information. Using positional embedding (Vaswani et al., 2017; Gao et al., 2019) to provide original relative position information might be a potential alternative to BiLSTM, which we leave to the future work.

### 5.2 Performance against Input Length

We follow Song et al. (2018) to conduct analysis to study the model performance against input length. Figure 4 shows the performance of MrGCN under different sentence lengths. In *n*-ary dataset, the performance differences between models with and without pooling gradually increase when the input sentences grow longer. Similarly, in the CDR dataset, the performance difference reaches 5.4 F1

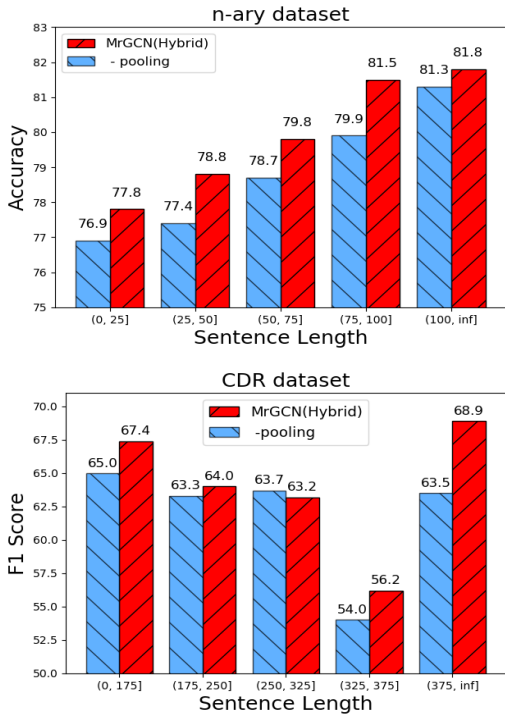


Figure 4: Performance against input length.

scores when the text length is over 375 tokens, while the difference is not significant when the input sentence is less than 325 words. This further demonstrates that the pooling-unpooling mechanism helps cases with longer context.

We have observed that in CDR dataset, MrGCN suffers from a performance drop on instances with sentence length between 325 and 375. Also, there are no significant performance differences under different sentence length for MrGCN without pooling. It is counterintuitive that we assume lengthier instances should be harder for models and usually have lower performances. One hypothetical reason is our way of model selection. Specifically, we select the model according to the overall performance, hence, the final model can possibly be biased towards the instances with sentence length more than 375<sup>7</sup>. The other hypothesis is that sentence length is not a good enough indicator to judge an input instance requiring long-term dependencies or not. In some cases, although their input texts are long, the designated entities are neighboring, hence, they are less in demand for long-term dependencies. To better study the long-term dependency requirements, we propose to study the model performance against entity distances.

<sup>7</sup>The hypothesis can also explain the phenomenon in Fig. 5

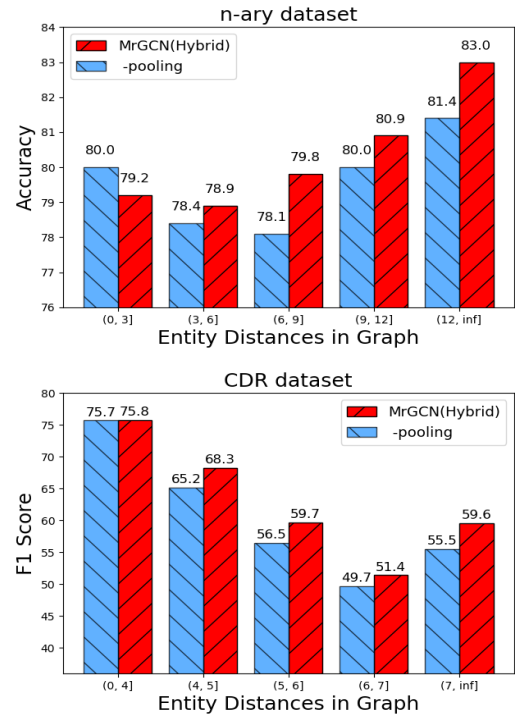


Figure 5: Performance against entity distance in graph.

### 5.3 Performance against Entity Distance

To better estimate the dependencies between entities for making a relation prediction, we categorize each instance based on its entity distance in the document graph. For mention-centric RE, we calculate the minimum distance between mentions in the graph<sup>8</sup>. In the ternary relation, we take the maximum among the three mention pair distances to provide the upper-bound estimation. Similarly, for entity-centric RE, we first calculate the minimum distance between each targeted mention pairs in the input graph, and then take the maximum over all mention pairs to be the entity distance.

Figure 5 shows the result of MrGCN under different entity distance in graph. We can observe that the performances for both models degrade significantly in CDR when the entity distance increases. In *n*-ary dataset, unlike Figure 4, the performances for model without pooling do not increase as the entity distance grow. These fact indicate that the entity distance properly measures the difficulty of an instance. However, with the help of graph pooling, MrGCN(Hybrid) consistently outperforms MrGCN(Hybrid)-pooling when the entity distance is larger than 4 in CDR, 3 in *n*-ary, which also supports our claims on the effectiveness of using

<sup>8</sup>If mentions contain multiple tokens, we calculate the average distances between each token pairs.

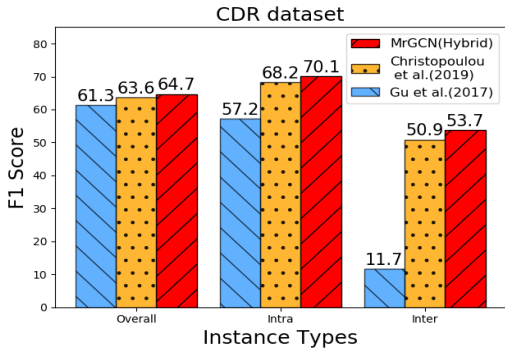


Figure 6: The results show the F1 results (%) on the CDR test set for different groups.

graph pooling to better learn representations for long-term dependencies.

#### 5.4 Results against Instance Types on CDR

Gu et al. (2017) pooled the instances in CDR dataset into two groups at intra- and inter-sentence level. The former means a mention pair is within the same sentence, while the latter means otherwise. Figure 6 presents the performance of MrGCN(Hybrid) under these different cases, and we can see that our method performs better on both pairs and the improvements on inter-sentence pairs are larger than intra ones, which is the same phenomenon observed from the  $n$ -ary dataset. These observations support that our model is capable of modeling complex inputs with longer context.

## 6 Related work

**Relation Extraction Beyond Single Sentence.** Peng et al. (2017) extend traditional RE to discerning the relation between  $n$  ( $n \geq 2$ ) entities in the cross sentence scenario, and use two graph LSTM to encode the full document graph. However, information may be lost by dividing the whole graph into two halves. Song et al. (2018) applies graph convolution on the entire graph, yet the receptive field scale in the method merely allows each graph node to see information within 5-hop distances at most, which limits the representation learning. *Soft pruning* strategy from (Guo et al., 2019) forces each node to connect all other nodes using virtual edges. This ignores the original structural information of the input graph. MrGCN not only enlarges the receptive field scale but also maintains the graph structure information.

Another thread of related works is the entity-centric relation extraction on the document-level.

Prior works (Gu et al., 2016, 2017) learn document-level RE using different models for intra- and inter-sentence instance. Recently, Sahu et al. (2019) build a labelled edge GCN model to use non-local dependencies presented in document graph to perform document-level RE. However, they directly apply vanilla GCN without specifically-designed model structure to handle long-term dependencies. Additionally, Jia et al. (2019) propose a multi-scale representation learning approach, where final entities representation is merged from many smaller contexts embedding. Christopoulou et al. (2019) use rules to build edge representation from nodes and perform relation prediction based on edges. Our method can be further migrated to enhance both their frameworks, since we focus on learning better node representations handling long-term dependencies.

**Graph Pooling in NLP.** Graph pooling is a classic idea to learn representation associated with graph and can largely preserve the graph structure (Duvenaud et al.; Simonovsky and Komodakis, 2017; Fey et al., 2018; Chen et al., 2018a). There are a few works that leverage the idea of graph pooling for NLP tasks. (Gao et al., 2019) adopts graph pooling to aggregate all local features for global text representation, via an “asymmetric” architecture without the unpooling operation, which differs from our work. Nguyen and Grishman (2018) has also explored the idea of pooling with GCN, but their pooling is conducted on layer-wise output features instead of input graph. To the best of our knowledge, we are the first to apply idea of graph pooling on RE.

**Pooling-unpooling Mechanism.** The pooling-unpooling mechanism is widely-used for pixel-wise representation learning (Ronneberger et al., 2015; Badrinarayanan et al., 2017; Chen et al., 2018b; Milletari et al., 2016), which utilize down-sampling and upsampling operation to aggregate information from different resolution inputs. The wide usage of such mechanism also is due to the popularity of deep learning application (Guo and Choi, 2019; Guo et al., 2020; Xie et al., 2020). The flagship work of such paradigm is U-Net (Ronneberger et al., 2015), which demonstrates the effectiveness in the image segmentation. It is worth mentioning that Gao and Ji (2019) adopts such paradigm for graph node and graph classification task, and share with our work similarity from the architectural perspective. However, the main con-

tribution of them is the specially-designed pooling and unpooling operations that suit for U-shape GCN. In contrast, our work focuses the effectiveness of such symmetric architecture in RE with long-term dependencies, also compatible with different general graph pooling method.

## 7 Conclusion

In this work, we explore the effectiveness of applying graph pooling-unpooling mechanism for representation learning in the NLP domain with RE applications. The idea of graph pooling helps the model learn larger receptive fields for graph nodes and achieve better performances in tasks which require learning long-term dependencies.

Also, we leave two potential directions for the future work. First, the proposed framework can be easily adapted to other NLP tasks that require capturing long-term dependencies. Second, our model is agnostic to the graph pooling method. We plan to investigate graph pooling methods that are specifically designed for NLP tasks and improve the current results.

## References

Kosuke Akimoto, Takuya Hiraoka, Kunihiko Sadamasa, and Mathias Niepert. 2019. *Cross-sentence n-ary relation extraction using lower-arity universal schemas*. In *Proceedings of the 2019 Conference on Empirical Methods in Natural Language Processing and the 9th International Joint Conference on Natural Language Processing (EMNLP-IJCNLP)*, pages 6224–6230, Hong Kong, China. Association for Computational Linguistics.

Vijay Badrinarayanan, Alex Kendall, and Roberto Cipolla. 2017. Segnet: A deep convolutional encoder-decoder architecture for image segmentation. *IEEE transactions on pattern analysis and machine intelligence*, 39(12):2481–2495.

Joost Bastings, Ivan Titov, Wilker Aziz, Diego Marcheggiani, and Khalil Sima'an. 2017. Graph convolutional encoders for syntax-aware neural machine translation. *arXiv preprint arXiv:1704.04675*.

Haochen Chen, Bryan Perozzi, Yifan Hu, and Steven Skiena. 2018a. Harp: Hierarchical representation learning for networks. In *AAAI*.

Liang-Chieh Chen, Yukun Zhu, George Papandreou, Florian Schroff, and Hartwig Adam. 2018b. Encoder-decoder with atrous separable convolution for semantic image segmentation. In *Proceedings of the European conference on computer vision (ECCV)*, pages 801–818.

Billy Chiu, Gamal Crichton, Anna Korhonen, and Sampo Pyysalo. 2016. How to train good word embeddings for biomedical nlp. In *Proceedings of the 15th workshop on biomedical natural language processing*, pages 166–174.

Fenia Christopoulou, Makoto Miwa, and Sophia Ananiadou. 2019. *Connecting the dots: Document-level neural relation extraction with edge-oriented graphs*. In *Proceedings of the 2019 Conference on Empirical Methods in Natural Language Processing and the 9th International Joint Conference on Natural Language Processing (EMNLP-IJCNLP)*, pages 4925–4936, Hong Kong, China. Association for Computational Linguistics.

Allan Peter Davis, Cynthia J Grondin, Robin J Johnson, Daniela Sciaky, Roy McMorran, Jolene Wiegers, Thomas C Wiegers, and Carolyn J Mattingly. 2019. The comparative toxicogenomics database: update 2019. *Nucleic acids research*, 47(D1):D948–D954.

David K Duvenaud, Dougal Maclaurin, Jorge Iparraguirre, Rafael Bombarell, Timothy Hirzel, Alán Aspuru-Guzik, and Ryan P Adams. Convolutional networks on graphs for learning molecular fingerprints. In *NeurIPS*.

Matthias Fey, Jan Eric Lenssen, Frank Weichert, and Heinrich Müller. 2018. Splinecnn: Fast geometric deep learning with continuous b-spline kernels. In *CVPR*.

Hongyang Gao, Yongjun Chen, and Shuiwang Ji. 2019. Learning graph pooling and hybrid convolutional operations for text representations. In *The World Wide Web Conference*, pages 2743–2749.

Hongyang Gao and Shuiwang Ji. 2019. Graph u-nets. *arXiv preprint arXiv:1905.05178*.

Jinghang Gu, Longhua Qian, and Guodong Zhou. 2016. Chemical-induced disease relation extraction with various linguistic features. *Database*, 2016.

Jinghang Gu, Fuqing Sun, Longhua Qian, and Guodong Zhou. 2017. Chemical-induced disease relation extraction via convolutional neural network. *Database*, 2017.

Xiao Guo and Jongmoo Choi. 2019. Human motion prediction via learning local structure representations and temporal dependencies. In *Proceedings of the AAAI Conference on Artificial Intelligence*, volume 33, pages 2580–2587.

Xiao Guo, Hengameh Mirzaalian, Ekraam Sabir, Aysush Jaiswal, and Wael Abd-Almageed. 2020. Cord19sts: Covid-19 semantic textual similarity dataset. *arXiv preprint arXiv:2007.02461*.

Zhijiang Guo, Yan Zhang, and Wei Lu. 2019. Attention guided graph convolutional networks for relation extraction. *ACL*.

Pankaj Gupta, Subburam Rajaram, Hinrich Schütze, and Thomas Runkler. 2019. Neural relation extraction within and across sentence boundaries. In *Proceedings of the AAAI Conference on Artificial Intelligence*, volume 33, pages 6513–6520.

Kaiming He, Xiangyu Zhang, Shaoqing Ren, and Jian Sun. 2016. Deep residual learning for image recognition. In *CVPR*, pages 770–778.

Robin Jia, Cliff Wong, and Hoifung Poon. 2019. Document-level  $n$ -ary relation extraction with multiscale representation learning. *arXiv preprint arXiv:1904.02347*.

Thomas N Kipf and Max Welling. 2016. Semi-supervised classification with graph convolutional networks. *ICLR*.

Yann LeCun, Léon Bottou, Yoshua Bengio, Patrick Haffner, et al. 1998. Gradient-based learning applied to document recognition. *Proceedings of the IEEE*, 86(11):2278–2324.

Junhyun Lee, Inyeop Lee, and Jaewoo Kang. 2019. Self-attention graph pooling. *arXiv preprint arXiv:1904.08082*.

Jiao Li, Yueping Sun, Robin J Johnson, Daniela Sciaky, Chih-Hsuan Wei, Robert Leaman, Allan Peter Davis, Carolyn J Mattingly, Thomas C Wiegers, and Zhiyong Lu. 2016a. Biocreative v cdr task corpus: a resource for chemical disease relation extraction. *Database*, 2016.

Zhiheng Li, Zhihao Yang, Hongfei Lin, Jian Wang, Yingyi Gui, Yin Zhang, and Lei Wang. 2016b. Cidextractor: A chemical-induced disease relation extraction system for biomedical literature. In *2016 IEEE International Conference on Bioinformatics and Biomedicine (BIBM)*, pages 994–1001. IEEE.

Jiongqian Liang, Saket Gurukar, and Srinivasan Parthasarathy. 2018. Mile: A multi-level framework for scalable graph embedding. *arXiv preprint arXiv:1802.09612*.

Wenjie Luo, Yujia Li, Raquel Urtasun, and Richard Zemel. 2016. Understanding the effective receptive field in deep convolutional neural networks. In *Advances in neural information processing systems*, pages 4898–4906.

Christopher D. Manning, Mihai Surdeanu, John Bauer, Jenny Finkel, Steven J. Bethard, and David McClosky. 2014. The Stanford CoreNLP natural language processing toolkit. In *Association for Computational Linguistics (ACL) System Demonstrations*, pages 55–60.

Diego Marcheggiani and Ivan Titov. 2017. Encoding sentences with graph convolutional networks for semantic role labeling. *EMNLP*.

Fausto Milletari, Nassir Navab, and Seyed-Ahmad Ahmadi. 2016. V-net: Fully convolutional neural networks for volumetric medical image segmentation. In *2016 Fourth International Conference on 3D Vision (3DV)*, pages 565–571. IEEE.

Mike Mintz, Steven Bills, Rion Snow, and Dan Jurafsky. 2009. Distant supervision for relation extraction without labeled data. pages 1003–1011. *ACL*.

Makoto Miwa and Mohit Bansal. 2016. End-to-end relation extraction using lstms on sequences and tree structures. *arXiv preprint arXiv:1601.00770*.

Dat Quoc Nguyen and Karin Verspoor. 2018. Convolutional neural networks for chemical-disease relation extraction are improved with character-based word embeddings. *arXiv preprint arXiv:1805.10586*.

Thien Huu Nguyen and Ralph Grishman. 2018. Graph convolutional networks with argument-aware pooling for event detection. In *Thirty-second AAAI conference on artificial intelligence*.

Adam Paszke, Sam Gross, Francisco Massa, Adam Lerer, James Bradbury, Gregory Chanan, Trevor Killeen, Zeming Lin, Natalia Gimelshein, Luca Antiga, Alban Desmaison, Andreas Kopf, Edward Yang, Zachary DeVito, Martin Raison, Alykhan Tejani, Sasank Chilamkurthy, Benoit Steiner, Lu Fang, Junjie Bai, and Soumith Chintala. 2019. Pytorch: An imperative style, high-performance deep learning library. In *Advances in Neural Information Processing Systems 32*, pages 8024–8035.

Nanyun Peng, Hoifung Poon, Chris Quirk, Kristina Toutanova, and Wen-tau Yih. 2017. Cross-sentence  $n$ -ary relation extraction with graph lstms. *Transactions of the Association for Computational Linguistics*.

Yifan Peng, Chih-Hsuan Wei, and Zhiyong Lu. 2016. Improving chemical disease relation extraction with rich features and weakly labeled data. *Journal of cheminformatics*, 8(1):53.

Jeffrey Pennington, Richard Socher, and Christopher Manning. 2014. Glove: Global vectors for word representation. In *Proceedings of the 2014 conference on empirical methods in natural language processing (EMNLP)*, pages 1532–1543.

Chris Quirk and Hoifung Poon. 2016. Distant supervision for relation extraction beyond the sentence boundary. *EACL*.

Olaf Ronneberger, Philipp Fischer, and Thomas Brox. 2015. U-net: Convolutional networks for biomedical image segmentation. In *International Conference on Medical image computing and computer-assisted intervention*, pages 234–241. Springer.

Sunil Kumar Sahu, Fenia Christopoulou, Makoto Miwa, and Sophia Ananiadou. 2019. Inter-sentence relation extraction with document-level graph convolutional neural network. In *Proceedings of the*

57th Annual Meeting of the Association for Computational Linguistics, pages 4309–4316, Florence, Italy. Association for Computational Linguistics.

Martin Simonovsky and Nikos Komodakis. 2017. Dynamic edge-conditioned filters in convolutional neural networks on graphs. In *CVPR*, pages 3693–3702.

Linfeng Song, Yue Zhang, Zhiguo Wang, and Daniel Gildea. 2018. N-ary relation extraction using graph state lstm. *EMNLP*.

Yoshimasa Tsuruoka, Yuka Tateishi, Jin-Dong Kim, Tomoko Ohta, John McNaught, Sophia Ananiadou, and Jun’ichi Tsujii. 2005. Developing a robust part-of-speech tagger for biomedical text. In *Panhellenic Conference on Informatics*, pages 382–392. Springer.

Ashish Vaswani, Noam Shazeer, Niki Parmar, Jakob Uszkoreit, Llion Jones, Aidan N Gomez, Łukasz Kaiser, and Illia Polosukhin. 2017. Attention is all you need. In *Advances in neural information processing systems*, pages 5998–6008.

Patrick Verga, Emma Strubell, and Andrew McCallum. 2018. Simultaneously self-attending to all mentions for full-abstract biological relation extraction. In *Proceedings of the 2018 Conference of the North American Chapter of the Association for Computational Linguistics: Human Language Technologies, Volume 1 (Long Papers)*, pages 872–884, New Orleans, Louisiana. Association for Computational Linguistics.

Hanchen Xie, Mohamed E Hussein, Aram Galstyan, and Wael Abd-Almageed. 2020. Muscle: Strengthening semi-supervised learning via concurrent unsupervised learning using mutual information maximization. *arXiv preprint arXiv:2012.00150*.

Zhitao Ying, Jiaxuan You, Christopher Morris, Xiang Ren, Will Hamilton, and Jure Leskovec. 2018. Hierarchical graph representation learning with differentiable pooling. In *NeurIPS*.

Bing Yu, Haoteng Yin, and Zhanxing Zhu. 2019. St-unet: A spatio-temporal u-network for graph-structured time series modeling. *arXiv preprint arXiv:1903.05631*.

Yuhao Zhang, Peng Qi, and Christopher D Manning. 2018. Graph convolution over pruned dependency trees improves relation extraction. *EMNLP*.

## A Dataset Details

### A.1 $n$ -ary dataset

The statistics of the  $n$ -ary dataset is presented in Table 4 and Table 5. We can see that most of the instances contain multiple sentences. Data is categorized with 5 classes: “resistance or non-response”, “sensitivity”, “response”, “resistance”, and “None”. Following prior works, we consider the binary detection task by treating all relation labels except “None” as True.

### A.2 CDR dataset

We adapt our data-preprocessing from the source released by Christopoulou et al. (2019)<sup>9</sup>. The statistics is presented in Table 6. We follow (Gu et al., 2017), (Verga et al., 2018) and (Christopoulou et al., 2019) to ignore non-related pairs that correspond to general concepts (MeSH vocabulary hypernym filtering). More details can refer to (Gu et al., 2017).

## B Experiment Details

### B.1 $n$ -ary dataset

#### B.1.1 Model architecture

The word vector is initialized by GloVe, 300 feature dimensions. We further concatenate it with 30-dimensional POS tag embedding before feeding into the Bi-LSTM layer. All these vectors will be updated during training. We use one layer Bi-LSTM with 330 hidden dimensions and each GCN

<sup>9</sup><https://github.com/fenchri/edge-oriented-graph>

Folds	Binary	Ternary
fold#0	1256	1474
fold#1	1180	1432
fold#2	1234	1252
fold#3	1206	1531
fold#4	1211	1298

Table 4: The detailed distribution of data instances over the 5-fold on the  $n$ -ary dataset. The data partitioning is provided from the original dataset.

Data	Avg. Token	Avg. Sent.	Cross
Ternary	73.0	2.0	70.1%
Binary	61.0	1.8	55.2%

Table 5: The  $n$ -ary dataset statistics. Avg. Token and Avg. Sent. are the average number of tokens and average sentence length per instance. Cross means the percentage of instance that contains two or more sentences.

	Train	Dev	Test
Documents	500	500	500
Positive pairs	1038	1012	1066
Intra	754	766	747
Inter	284	246	319
Negative pairs	4202	4075	4138
Entities			
Chemical	1467	1507	1434
Disease	1965	1864	1988
Mentions			
Chemical	5162	5307	5370
Disease	4252	4328	4430
Avg sent. len./doc.	25.6	25.4	25.7
Avg sents./doc.	9.2	9.3	9.7

Table 6: CDR dataset statistics

Attention head	4, 8, 10, <b>20</b> , 25
Batch size	4, <b>8</b> , 12, 16, 24, 32
Sublayer ( $S$ )	2 3 4
Level ( $L$ )	2 3 4

Table 7: The searching space for hyper-parameters for  $n$ -ary dataset. The bold means the best head number for multi-head self-attention and the batch size. The sublayer ( $S$ ) and level ( $L$ ) are different for each task in the  $n$ -ary dataset.

layer contains 200 hidden nodes. Dropout layers are used to prevent overfitting and set to 0.5.

### B.1.2 Hyper-parameters

The learning rate of our SGD optimizer is initialized at 0.1 with 0.95 decay after 15 epochs. All the models are set to train with 200 epochs with early stopping (20 epoch). It typically stops in less than 100 epochs. We first tune the attention head and batch size based on the development set performance on Ternary Detection, and select 20 heads for the multi-head self-attention and batch size equals to 8 as the final setup. Then we tune our main hyper-parameter — the number of GCN layers in GCN block ( $S$  in the main article, Sublayer in Table 7) and the number of pooling times ( $L$  in the main article, Level in Table 7) for each different tasks. The hyper-parameter searching space is listed in Table 7 and the best hyper-parameter for each model is stated in Table 8.

### B.2 CDR dataset

#### B.2.1 Model architecture

We follow Christopoulou et al. (2019) to use the PubMed pre-trained word embedding and fix it during training. The Bi-LSTM input will be the concatenation of word embedding and trainable POS-tag representations. The setup of the Bi-LSTM

	Detection		Classification		
	Ternary	Binary	Ternary	Binary	
CHM	L2S2	L2S4	L4S3	L2S3	
CHM-RNN	L3S2	L4S2	L2S2	L2S2	
Hybrid	L3S3	L2S2	L3S4	L2S2	
Hybrid-RNN	L4S2	L4S2	L4S2	L4S2	
Hybrid-Pool	20	14	15	15	
Hybrid-Pool-RNN	10	14	10	6	
Hybrid-Pool-Att.	10	15	12	6	

Table 8: The best Sublayer ( $S$ ) and Level ( $L$ ) for models in our main result and ablation studies for  $n$ -ary dataset. We use ‘‘Hybrid’’ to represent MrGCN(Hybrid) and ‘‘CHM’’ to replace MrGCN(CHM) in the table. The total number of GCN layers can be calculated by  $(2L - 1) \times S$ . For models without graph pooling, we list the total number of GCN layers we use.

	Layers	Epoch	Dev F1
MrGCN(Hybrid)	L3S4	55	66.0
-RNN	L4S4	58	64.6
-Pool	12	41	65.2
-RNN-Pool	6	97	63.9

Table 9: The best Sublayer ( $S$ ) and Level ( $L$ ) for each model in our main result and ablation studies on the CDR dataset. The total number of GCN layers can be calculated by  $(2L - 1) \times S$ . For models without graph pooling, we list the total number of GCN layers we use. We also report the epoch when each of our models gets its optimal development set performance.

layers, GCN layers, and dropout layer are the same as the setting in the  $n$ -ary dataset, except that we use two layers of Bi-LSTM rather than one.

### B.2.2 Hyper-parameters

The learning rate of the SGD optimizer for CDR dataset is set as 0.1 initially, and the learning rate will be decayed with scale 0.95 after 10 epochs. All the models are set to train with 200 epochs with the early stopping strategy, in which the patience is set as 15, but most of them stop around 60 epochs in the real case. We first decide the batch number by evaluating the performance on the development set, and get the best performance when the batch number is set with 16. We then train each ablation study model using the official training set and tune the sub-layer( $S$ ) and level( $L$ ) by the performance on the official development set. We use grid search to tune the sublayer from 3,4,5 and level from 2,3,4 if the experiment is with Graph Pooling. The best hyper-parameter is presented in Table 9.

$$\begin{aligned}
 A_0 &= \begin{bmatrix} n_0 & n_1 & n_2 & n_3 & n_4 & n_5 & n_6 & n_7 \end{bmatrix} = \begin{bmatrix} 0 & 1 & 0 & 0 & 0 & 0 & 0 & 0 \\ 1 & 0 & 1 & 0 & 1 & 0 & 0 & 0 \\ 0 & 1 & 0 & 0 & 0 & 0 & 0 & 0 \\ 0 & 0 & 0 & 0 & 1 & 0 & 0 & 0 \\ 0 & 1 & 0 & 1 & 0 & 1 & 0 & 0 \\ 0 & 0 & 0 & 0 & 1 & 0 & 1 & 1 \\ 0 & 0 & 0 & 0 & 1 & 0 & 1 & 1 \\ 0 & 0 & 0 & 0 & 0 & 1 & 0 & 1 \\ 0 & 0 & 0 & 0 & 0 & 1 & 1 & 0 \end{bmatrix} \\
 M_{0,1} &= \begin{bmatrix} m_0 & n_1 & m_1 & n_5 & m_2 \end{bmatrix} = \begin{bmatrix} 1 & 0 & 0 & 0 & 0 \\ 0 & 1 & 0 & 0 & 0 \\ 1 & 0 & 0 & 0 & 0 \\ 0 & 0 & 1 & 0 & 0 \\ 0 & 0 & 1 & 0 & 0 \\ 0 & 0 & 0 & 1 & 0 \\ 0 & 0 & 0 & 0 & 1 \\ 0 & 0 & 0 & 0 & 1 \end{bmatrix} \\
 A_1 &= M_{0,1}^T A_0 M_{0,1} = \begin{bmatrix} 0 & 2 & 0 & 0 & 0 \\ 2 & 0 & 1 & 0 & 0 \\ 0 & 1 & 2 & 1 & 0 \\ 0 & 0 & 1 & 0 & 2 \\ 0 & 0 & 0 & 2 & 2 \end{bmatrix}
 \end{aligned}$$

Figure 7: The matching matrix example.

## C Matching Matrices

In this section, we attach the example of matching matrix (as depicted in Figure 7) for Hybrid Matching mentioned in the Section 3.2.